Cyclones enhance the transport of sea spray aerosols to the high atmosphere in the Southern Ocean

Jun Shi[1,2], Jinpei Yan*[1,2], Shanshan Wang[1,2], Shuhui Zhao[3], Miming Zhang[1,2], Suqing Xu[1,2], Qi Lin[1,2], Hang Yang[1,2], Siying Dai[1,2]

[1]Key Laboratory of Global Change and Marine Atmospheric Chemistry, Ministry of Natural Resources, Xiamen 361005, China;

[2]Third Institute of Oceanography, Ministry of Natural Resources, Xiamen 361005, China.

[3]School of Tourism, Taishan University, Tai'an City, Shandong Province, China, 271000.

***Corresponding author：**

Jinpei Yan, Phone: 86-592-2099290, E-mail: jpyan@tio.org.cn

Address:No. 178Daxue Road, Siming District, Xiamen City, Fujian Province, China

Abstract： Cyclones are expected to increase the vertical transport of sea spray aerosols (SSAs), which may significantly impact the climate by increasing the cloud condensation nuclei (CCN)/cloud droplets (N_d) population, hence changing the radiation reflected back to space. In this study, high temporal resolution (1h) aerosol composition measurements were performed during a survey in the southern hemisphere middle and high latitudes during the period 23 February 2018 to 4 March 2018. The characteristics of SSAs during three cyclones were observed during the survey. The increase in wind speed during the cyclones had a minimal impact on the level of SSA, which deviates significantly from the anticipated scenario where higher wind speeds would lead to an increase in SSA concentration. However, the size of SSAs particles during the cyclones were larger than during the no-cyclone periods. It seems that the generation of SSAs is enhanced during cyclones, but SSAs concentration near the sea surface does not increase. Calculations suggest that more than 23% of SSAs can be transported upward during a cyclone period which can result in considerable quantities of SSAs being transported to high altitudes. The vertical transport also reduces the level of SSAs in the lower atmosphere. Additionally, the transport of SSAs to the high atmosphere during cyclones increases the CCN burden in the marine boundary layer. This study extends the knowledge of SSA generation and transport during cyclones, a large number of SSAs are transported to the upper air, the SSAs reaching high altitudes can change the radiation reflected back to space by modulating the CCN/N_d, which may impact the regional climate.

Keywords: Sea spray aerosols (SSAs), Cyclone, Southern Ocean, transport

1. Introduction

Sea spray aerosols (SSAs), one of the largest sources of primary aerosols in the marine atmosphere, makes a significant contribution to atmospheric aerosols and the primary inorganic sea salt component of SSAs dominates the marine aerosol mass size distribution (McInnes et al., 1996). It is reported that the annual global SSA flux is estimated to be 1.01×10^4 Tg yr^{-1} (Gong et al., 2002). Pure sea salt mostly consists of NaCl and a mixture of one or more other salts, such as Mg, K, Ca sulfates, and traces of organic material (Thomas et al., 2022). SSAs are considered to be the most important contributor to aerosol light scattering in the marine boundary layer (MBL) (Quinn and Coffman, 1999; Takemura et al., 2002). In addition, SSAs act as cloud condensation nuclei (CCN) (Pierce and Adams, 2006), thereby altering the reflectivity, lifetime and extent of clouds and hence further influence the global climate.

The influence of SSAs on cloud properties is thought to be particularly strong over remote ocean regions devoid of continental particles. For all supersaturations in the Southern Ocean (SO), SSA makes up more than 20% of the total CCN and up to 65% for low supersaturation, determined using a lognormal-mode-fitting procedure (Quinn et al., 2017). SSAs are formed predominantly by the action of the wind on the ocean (Stokes et al., 2013) as the major mechanism of SSA production is air bubbles bursting at the surface of the ocean as a result of wind stress (Monahan and Muircheartaigh, 1980). Wind stress on the ocean surface forms waves, bubbles are then formed and return to the surface, creating whitecaps and bursts, injecting sea water films and jet droplets into the atmosphere. Wind speed can also significantly affect the size distribution of SSAs (McDonald et al., 1982), although some studies have suggested that wind speed may not be the sole condition

affecting SSA production as humidity, temperature and sea-air temperature difference may also affect their formation (Cole et al., 2003; Shi et al., 2022; Liu et al., 2020). However, the production of SSAs in extreme weather (such as cyclones) in the southern hemisphere middle and high latitudes, especially in the SO, still remains uncertain.

Westerlies in the Southern Hemisphere fundamentally control regional patterns of air temperature while also regulating ocean circulation, heat transport, and carbon uptake (Goyal et al., 2021). Moreover, the zone of westerlies is prone to cyclones which dominate the precipitation pattern of the southern hemisphere mid-latitudes (Mycoy et al., 2020). The SO plays an important role in global carbon cycles and thus in climate change processes (Gruber et al., 2019). Furthermore, the SO is less affected by human activities and so the influence of SSAs on CCN is thought to be particularly strong over this region.

Cyclones can have great effect on marine aerosol, especially on SSAs in the atmosphere, as they may transport large water volumes and at the same time impose strong winds (Fang et al., 2009). Air convergence due to the reduction of pressure caused by cyclones may also affect SSA concentration. The study region typically experiences a higher frequency of cyclone development during the summer season compared to other seasons. It is reported that 959 cyclones occurred in the SO during the summer of 2004 to 2008 (Liu et al., 2012).

In summary, the impact of cyclones on the emission of SSAs cannot be ignored, SSAs can direct absorbing and scattering of solar radiation. What's more, Sea spray aerosol is an important source of CCN, which plays a significant role in regulating global warming, but it remains unclear how changes in cyclone occurrence can impact the emissions of SSAs. Due to the influence of CCNs, and hence SSAs, on related climatic processes, it is particularly important and timely to consider

this question although the lack of direct observations makes this challenging. As cyclones develop in the westerlies and the SO, the decrease of pressure, air convergence, strong winds and heavy precipitation may alter the emissions of SSAs and CCNs and thus affect regional climate in the mid and high latitudes of the southern hemisphere.

The observation of cyclones is commonly performed at fixed points on land (Badarinath et al., 2008), but such observations cannot be used to investigate the effect of cyclones on SSAs over remote ocean regions. However, continuous observation technology now available on research vessels can greatly improve the temporal and spatial resolution of SSA particle measurements, allowing for the in situ characterization of marine SSA behavior in extreme weather.

In this study, SSA characteristics were observed with high temporal resolution during three cyclones in the SO to determine the transport of SSAs upward to the high atmosphere by cyclones. The concentration and particle size of SSAs were measured simultaneously for the first time at high-temporal resolution (1h) in the southern hemisphere mid and high latitudes during three cyclones (23 February to 4 March 2018). The results provide a new insight into the effect of cyclones on the generation and vertical transport of SSAs in the mid and high latitudes of the SO.

2. Methodology

2.1 Observational sites

Observations were carried out on board the R/V “Xuelong” during the 34th Chinese Antarctica Expedition Research Cruise. This survey covered with a large portion of the SO (40°S to 73°S, 170°E to 124°W, Fig. S1). The observations presented here were obtained between 23 February and 4 March 2018.

2.2 SSA measurement

Aerosol composition, including sea salts, were monitored at a temporal resolution of 1 h using an in situ gas and aerosol composition monitoring system (IGAC, Model S-611 http://www.machine-shop.com.tw/). To minimize the impact of ship emissions, the sampling inlet connected to the monitoring instruments was fixed 20 m above the sea surface on a mast located at the bow of the research vessel. Note that the major pollution source is from the chimney, which is located at the stern of the R/V and about 25 meters above the sea level. Hence, the pollution emissions from the vessel mainly located at the downwind of the sampling inlet, especially when the vessel is running. As high-time-resolution observations are used in this study, the self-contaminations from the vessel have been eliminated from the measurement results. The wind speed and wind directions were also monitoring during the observation period, which were used to determine if the observations were affected by the self-contaminations or not. The data have been corrected to eliminate the impact of ship contamination in this study. A total suspended particulate sample inlet was also positioned at the top of the mast. All aerosol observational instruments were connected by conductive silicone tubing with an inner diameter of 1.0 cm.

The IGAC monitoring system consisted of three main units, including a Wet Annular Denuder (WAD), a Scrub and Impact Aerosol Collector (SIAC), and an ion chromatograph with a sampling flow of 16.7 LPM. On the one hand, the collection of acidic and basic gases relies on the diffusion and absorption of gases into a downward flowing aqueous solution. and was positioned at an angle to facilitate the collection of enlarged particles. On the other hand, ultrapure water was fed continuously into the nozzle at 1.2 mL/min and heated to 140 °C to vaporize the water. Steam was sprayed directly towards the particle-laden air to improve the humidity of the flue gases. Fine

particles were enlarged and subsequently accelerated through a conical-shaped impaction nozzle and collected on the impaction plate. The gas and aerosol liquid samples from the WAD and SIAC were drawn separately by a pair of syringe pumps, where one syringe collected the current sample (55 min) and the other injected the previous sample. The samples were then subsequently analyzed for anions and cations by an online ion chromatography (IC) system (Dionex ICS-3000). The injection loop size was 500 L for both anions and cations. (Young et al., 2016). Six to eight concentrations of standard solutions were used for calibration purposes, depending on the target concentration (R^2 values above 0.997). The detection limits for Na^+ concentration was 0.03 μg L^{-1} (aqueous solution).

2.3 SSA particle size measurement

A single particle mass spectrometer (SPAMS) was used to measure the SSA particle size distribution. A Nafion tube dryer was placed before the SPAMS to remove the moisture of sampling gas. Details of the methods used for aerosol detection and the operational procedure for the on-board SPAMS have been presented in a previous study (Li et al., 2014).

The measurement of particle size distribution using SPAMS has been confirm in previous studies (Yan et al., 2016; Li et al., 2014; Ma et al; 2016). A PM2.5 collector was deployed to remove particles larger than 2.5 μm. Fine particles were drawn into the vacuum system through a critical orifice and were then accelerated and focused to form a particle beam. Particles with specific velocities then passed through two continuous diode Nd:YAG lasers (532 nm). The aerodynamic diameter of a single particle was calculated using the particle velocity. The particle sizes detected by the SPAMS were calibrated using polystyrene latex spheres (PSL, Duke Scientific Corp., Palo

Alto) with diameters of 0.2, 0.3, 0.5, 0.75, 1.0, 2.0, and 2.5 μm (Li et al., 2011).

2.4 Meteorological parameters

Meteorological parameters such as wind speed (WS) and temperature were measured continuously using an automated meteorological station mounted on the R/V “Xuelong". The time resolution of the meteorological data is 1 hr. Weather map data, including sea surface pressure and total precipitation, was obtained from the fifth generation ECMWF reanalysis for the global climate and weather (ERA5. https://cds.climate.copernicus.eu/). Satellite cloud maps were obtained from the Level-1 and Atmosphere Archive and Distribution System Distributed Active Archive Center (LAADS DAAC data product MOD021KM. https://ladsweb.modaps.eosdis.nasa.gov/).

2.5 Undisturbed SSA concentration estimates during the cyclone period

Undisturbed SSA (U-SSA)stand for the SSA concentration in the case of no cyclone disturbance which estimated by the differences of wind stress or sea-salt flux between cyclone and non-cyclone periods. U-SSA concentrations during the cyclone period were estimated in the following two ways.

The momentum flux at the air-sea interface, also called wind stress, is an important part of the interaction between ocean and atmosphere and reflects the friction and drag effect between the two fluids. Wind stress is the energy source of SSA formation. The momentum flux at the air-sea interface can be calculated using the equation (1) (Toffoli et al., 2012):

$$\tau = \rho_a C_d U_{10}^2 \quad (1)$$

where $\rho_a$is the air density, U_{10} is the wind speed as measured at 10 m above the mean water level, and C_d is a drag coefficient which can be expressed as follows:

$$C_d = (a + bU_{10}) \times 10^{-3} \quad (2)$$

where a is 0.96 and b is 0.06.

By means of comparing the difference of wind stress between cyclonic and non-cyclonic periods and combining with the concentration of SSAs during non-cyclonic periods to obtained U-SSA $_{(\text{wind stress})}$ concentration.

$$\text{U-SSA}_{(\text{wind stress})} = \frac{\tau_{\text{cy}}}{\tau_{\text{non-cy}}} * \text{SSA}_{(\text{non-cy})} \quad (3)$$

For the indirect production of SSAs through the formation and bursting of bubbles, the SSA flux function dF_0/dr (particles m^{-2} s^{-1} mm^{-1}) which expresses the rate of sea water droplet generation per unit area of sea surface per increment of particle radius, is given by Monahan et al. (1986) as Eq. (4):

$$\text{SSA flux} = \frac{dF_0}{dr} = 1.373 U_{10}^{3.41} r^{-3} (1 + 0.057 r^{1.05}) \times 10^{1.19 e^{-B^2}} \quad (4)$$

where $B = (0.38 - \log r)/0.65$, r is the particle radius and U_{10} is as defined above.

U-SSA $_{(\text{Sea-salt flux})}$ concentration can be obtained as follows:

$$\text{U-SSA}_{(\text{Sea-salt flux})} = \frac{\text{SSA flux}_{\text{cy}}}{\text{SSA flux}_{\text{non-cy}}} * \text{SSA}_{(\text{non-cy})} \quad (5)$$

3. Results and discussion

3.1 Meteorology

The observational campaign was carried out from 23 February to 4 March 2018. The study area is noted for the influence of cyclones and was defined by the outermost closed isobar surrounding the cyclone area center (Wernli and Schwierz, 2006). Rainfall affects numerous aspects of SSA production. Under certain conditions, raindrops falling onto the sea surface can produce SSA particles directly or indirectly, either from bubbles entrained by the drop or from bubbles or SSA particles produced by the splashed drops resulting from the original impact (Blanchard and Woodcock, 1957). However, falling raindrops can also function as efficient scavengers of particles

in the atmosphere (Lewis and Schwartz, 2004). We therefore extracted data from periods of precipitation during the cruise. Although relative humidity can affect SSA production, relative humidity is higher on the ocean than on land which basically reached the deliquescence point (about RH:75%) of NaCl (Cole et al, 2003) in the study period. In this case, the change of relative humidity has little influence on the change of particle size. Three cyclone events were captured during this period (Fig. S2). Na^+ derived from SSA is an important component of marine atmospheric aerosols (Teinila et al., 2014) and is generally considered to be a marker of SSAs in the marine atmosphere (Yeatman et al., 2001). Hence, Na^+ concentrations and meteorological information from the study period are presented in Fig. 1.

The R/V "Xuelong" started from 173°E 44°S and sailed due south, encountering a cyclone which was generated at about 150°E, gradually moving eastwards (Fig. 2). As the cyclone approached, the research vessel sampled a northwest warm and humid air mass followed by precipitation. As the research vessel entered the cyclone area (Event 1. See shaded area, Fig. 1) at about 15:00 24/2/18 (all times presented here are UTC), air pressure suddenly dropped (from 1003 hpa to 961 hpa) and wind speed significantly stronger than in the non-cyclone area was experienced (average wind speed increased from 11.7 m s^{-1} to 14.8 m s^{-1}). However, the average Na^+ concentration during this cyclone event remained relatively constant as the WS increased, changing from 1529 ng m^{-3} to 1706 ng m^{-3}. At about 23:00 25/2/18, the research vessel left the cyclone area. Note that wind speed dropped sharply between 13:00 and 23:00 25/2/18 (average 14.8 ms^{-1} and 9.3 ms^{-1}, respectively) and this was matched by a rapid decrease in SSA concentrations (from 1706 ng m^{-3} to 343 ng m^{-3}. Fig. 1b).

As the vessel continued to move south it encountered another cyclone area at 10:00 26/2/18

and immediately turned to the southeast, leaving the cyclone area at 22:00 26/2/18 (Event 2. Shaded area Fig. 1). During Event 2, the research vessel did not pass through the center of the cyclone. However, the observed atmospheric pressure dropped from 983 hpa to 973 hpa and the average wind speed increased from 13.5 m s^{-1} to 15.5 m s^{-1}. Similar to Event 1, the average Na^+ concentration during the cyclone period remained relatively constant, or even decreased (from 2810 ng m^{-3} to 2354 ng m^{-3}), as the WS increased. The dominant air flow was cold and westerly thus there was only a little precipitation (Fig. 2).

While the research vessel moved southeast and deep into the SO, Na^+ concentrations were much lower than during the first two cyclone events, which suggested that low air temperatures and sea ice cover reduces the production of SSAs (Fig. S3) (Yan et al., 2020). Between 18:00 1/3/18 and 04:00. 4/3/18, the research vessel encountered a third cyclone (Event 3). The wind speed increased from 7.5 m s^{-1} to 21.5 m s^{-1} and the air pressure dropped from 986 hpa at its highest to 960 hpa at its lowest. Similarly, the average Na^+ concentration during this cyclone period did not increase significantly (changed from 255 ng m^{-3} to 335 ng m^{-3}). The cyclone encountered during Event 3 was relatively stable and moved slowly, and there was only a small amount of precipitation generated in the wind shear region.

3.2 SSA concentration

Correlation Coefficients Between element of Sea Spray Aerosol in the Atmospheric Aerosols Recorded in This Study have shown in Table S1. Na^+ have high correlation with Mg^{2+}, K^+, Ca^{2+} and SO_4^{2-}, implying Na^+ has a good representation of SSA. The variation of Na^+ concentrations in regions of different latitude are presented in Fig. S4 (Supplementary Material). Positive correlations

between Na^+ concentrations and wind speeds were found in the low-middle latitudes (20°N- 40°S) (R=0.59, Fig.S4), where the change of atmospheric pressure was small (Fig. S5). This suggests that that SSA generation was greatly influenced by the wind speed. However, correlations between Na^+ concentrations and wind speeds were relatively low in middle-high latitudes (40°S-60°S) and in the polar region (60°S-74°S) (R=0.45 and 0.05, respectively), where the change of pressure was highly variable (Fig. S5), suggesting that the cyclones may have affected the relationship between wind speed and SSA concentrations in the MBL, further resulting in climate effects.

To further investigate the influence of southern hemisphere middle and high latitude cyclones on SSA concentrations, a non-cyclone "normal" period (5 and 6 April), which had stable pressure and relative humidity controlled by a constant air mass with no precipitation, was selected as a control period. The relationship between WS and Na^+ concentrations under different meteorological conditions are illustrated in Fig. 3.

It is readily apparent that the Na^+ concentration, and hence the concentration of SSAs, increased as the WS increased during the control period (Fig. 3a, R = 0.74). Positive correlations between Na^+ concentrations and WS were also present during periods of non-cyclone during the three events (R = 0.65, 0.64 and 0.50, respectively), which is in reasonable agreement with previous studies (e.g., O'Dowd and de Leeuw, 2007). It is worth noting here that the correlations between Na^+ concentrations and WS during Event 3 were lower than during the other two events. This may be due to the lower temperatures and sea ice cover there, weakening the influence of WS on SSA production (Yan et al., 2020).

In contrast, the correlations between Na^+ concentration and wind speed are much lower during all three cyclone periods (R = -0.32, 0.15 and 0.44) and precipitation periods (R = 0.08 and -0.02.

Fig. 3b, 3c and 3d). During the cyclone periods, Na^+ concentrations changed irregularly as the WS increased, suggesting that rainfall was altering the influence of wind stress on SSA production. This implies that the effect of precipitation on the formation of SSA is complicated and that under this circumstance, WS may not be the critical factor that affects SSAs emission. Further studies of how SSA concentrations change during precipitation periods are required.

During the cyclone periods which had strong WSs, we did not observe obvious correlations between WS and Na^+ concentration. Some Na^+ concentrations during cyclone periods were even lower than those during non-cyclone periods. This suggested that, although there were stronger WSs, the low pressure caused by cyclones may transport a part of the SSA population upwards, producing more CCN at higher altitudes and simultaneously reducing the concentrations of Na^+ in the MBL. Another possibility is that the emission of SSAs during cyclonic periods may be lower than that in non-cyclone periods inherently. This is discussed further below.

3.3 SSA particle size distribution

Generally, SSA generation increases with wind speed, however in this study it has been found that higher wind speeds did not result in higher levels of SSAs during cyclone conditions. It seems that the generation of SSAs was suppressed during periods of cyclone. It is necessary to try to determine whether the emission of SSAs in the cyclonic periods was higher than that in the non-cyclone periods. Feng et al. (2017) and Liu et al. (2020) reported that both SSA particle size and the concentration increased with increasing wind speed. As the WS increased from 3.4 to 10 m s^{-1}, a 7–10 fold increase in atmospheric salt concentration was observed. Log-normal distributions predict a 30-fold increase in the concentration ($\mu g/m^3$) of particles larger than 1 x 10^{-9} g (10 μm radius) and

a 50-fold increase in the concentration of particles larger than 1 x 10^{-8} g (20 μm radius) (McDonald et al., 1982). If the particle sizes of SSAs increase with increasing wind speed, this indirectly confirms that the concentrations of SSAs also increase.

The size distributions of SSAs observed during the three cyclone events are presented in Table S2 and Fig. 4. During Event 1, the difference between the number of SSA particles larger than 1.2 μm observed in cyclone and non-cyclone periods was about 11%. The change of SSA size distribution during Event 2 and Event 3 were consistent with that during Event 1 (about 6% and 5%, respectively). The size spectrum of SSA particles changed toward larger sizes during cyclone periods during all three events. These results imply that cyclones in southern hemisphere middle and high latitudes enhance SSA generation. However, the increase of SSA concentrations was not present when high wind speeds occurred during cyclone periods, suggesting that SSAs may have been transported away from, or diluted in, the lower atmosphere.

3.4 Estimation of the proportion of SSAs transported upward by cyclones

The middle and high latitude of southern hemisphere especially the Antarctic region is one of the most pristine in the world and serves as an important proxy for the pre-industrial atmosphere. Human activity has little impact here and anthropogenic aerosols account for a small proportion of the total aerosol population. Aerosols are typically derived from natural sources, including primary particles (sea spray and bursting bubbles), which make up the vast majority of the aerosol mass. In this region cyclones tend to occur in summer, generating more SSAs due to high WS. However, our results suggest that air convergence caused by the cyclones may result in considerable quantities of SSAs being transported vertically to higher altitudes, which can partly explain why the mean

number concentration of CCN/cloud droplets (N_d) in the SO in summer is much higher than that in winter (Mycoy et al., 2020).

As mentioned above, the size of the sea salt particles was larger during cyclone events than that in no-cyclone period.. However, the level of SSA hardly increased with the wind speed during the cyclone processes. It's likely that there is a part of SSAs been transported upward by air convergence due to cyclone. The transport effect of updraft on SSAs on the one hand reduces the concentration of SSAs on the sea surface; On the other hand, a large number of SSAs are transported to the upper air, While the SSAs reaching high altitudes can change the radiation reflected back to space by modulating the N_d, which in turn changes cloud reflectivity even without any changes to cloud macrostructure (Twomey, 1977). Furthermore, by changing CCN/N_d, cloud microphysical processes are altered (Albrecht, 1989). These two effects, summarized in Fig. 5, can ultimately affect the radiation balance of the earth system in the mid and high latitudes of southern hemisphere (Quinn and Bates, 2011). Thus, the effect of cyclones on the production of SSAs, especially in the polar region, can not be neglected.

It is difficult to precisely estimate the proportion of SSAs transported vertically directly. However, the differences of wind stress or sea-salt flux between cyclone and non-cyclone periods can be calculated using the undisturbed concentrations of Na^+ (U-SSA concentration) during the cyclone period. This can be used to quantify the proportion of SSAs which may have been transported upward.

Fig. S6 and S7 shown the difference of wind stress and Sea-salt flux between cyclonic and non-cyclonic periods. The proportion of vertically transported SSAs, estimated using the wind stress method and the sea-salt flux method, are presented in Table 1. Using the wind stress method, more

than 23.4% of the SSAs were transported upward by cyclone processes during Event 1, and 36.2% and 38.9% in Event 2 and Event 3, respectively. The proportion of SSAs transported upwards estimated using the bubble method were higher than those estimated using the wind stress method for all three events. The transported proportion during Event 3, when the research vessel was located closer to the Antarctic, estimated using the bubble method was the highest, reaching 56.6%, which was much higher than that estimated for Event 1 (39.9%) or Event 2 (42.8%).

The high transportation ratio of Event 3 agrees with the results of a previous study which reported that the largest contribution of SSA to CCN (up to 65%) was observed in the high southern latitudes (Quinn et al., 2017). There may have been another factor affecting Event 3 results, as the research vessel was close to Antarctica where the WS was over 20 m s^{-1} for a few hours. However, as the sea state is typically not fully developed in such a situation, the energy flux from the air to the ocean may differ from that under steady state conditions, as may wave breaking and hence SSA production (Lewis and Schwartz, 2004). These circumstances can lead to the overestimation of the proportion of SSAs which are vertically transported. In summary, the results suggest that over the southern hemisphere middle and high latitudes, a significant proportion of SSAs are transported upward and subsequently potentially effect climate change processes.

The influence of cyclone on SSAs in the tropics, characterized by stronger and more intricate cyclonic system, is not covered by this paper. Further studies of how SSA concentrations change in tropical cyclone areas are required. However, the observational results presented in this study extend the current knowledge of how cyclones influence marine aerosol emissions in the southern hemisphere mid-and high-latitudes and their potential to alter climate change.

Conclusions

An underway aerosol monitoring system was used to determine the Na^+ concentration during different cyclone periods in southern hemisphere mid and high latitudes in order to access the potential effects of cyclone on SSA emissions. Three cyclones events were observed during the 34th Chinese Antarctica Expedition Research Cruise from 23 February 2018 to 4 March 2018.

It was expected that the high wind speeds produced during the cyclone events should have increased the generation of SSAs. However, although an increase in SSA particle size was observed, there were no obvious SSA concentration increases during these periods. It is likely that there was a proportion of the SSAs which were transported upward due to the cyclones. According to the wind stress and sea-salt flux between cyclone and non-cyclone periods, it was estimated that during cyclone periods, more than 23% of SSAs were transported upwards, with the highest proportion observed in the Southern Ocean (ranging from 39% to 55%). Vertically transported SSAs can be regarded as an important source of CCN and hence have an effect on climate in the mid and high latitudes of the southern hemisphere.

The effects of cyclones on SSA emissions are indirect and complicated. Therefore, future work should be carried out on the effect of cyclones of varying intensity on SSA emissions and their generation mechanism during periods of precipitation, as well as their potential climate effects at the different latitudes.

Acknowledgements

This study is financially supported by the Qingdao National Laboratory for Marine Science and Technology (No. QNLM2016ORP0109), the Natural Science Foundation of Fujian Province, China (No. 2019J01120), the Response and Feedback of the Southern Ocean to Climate Change (RFSOCC2020-2025), the Chinese Projects for Investigations and Assessments of the Arctic and

Antarctic (CHINARE2017-2020), and the National Natural Science Foundation of China (No. 41941014). The authors gratefully acknowledge the Guangzhou Hexin Analytical Instrument Company Limited for on-board observation technical assistance, and the Zhangjia Instrument Company Limited for IGAC technical assistance and data analysis.

Data availability

The data discussed in this manuscript are available from the following websites: https://doi.org/10.5281/zenodo.7912911.

Competing interests

The authors declare that they have no conflict of interest.

References

ALBRECHT, B. A. (1989). Aerosols, Cloud Microphysics, and Fractional Cloudiness. *Science,* 245(4923), 1227–1230. https://doi.org/10.1126/science.245.4923.1227

Badarinath, K. V. S., Kharol, S. K., Krishna Prasad, V., Kaskaoutis, D. G., &Kambezidis, H. D. (2008). Variation in aerosol properties over Hyderabad, India during intense cyclonic conditions. *International Journal of Remote Sensing, 29*(15), 4575-4597. https://doi.org/10.1080/01431160801950170

Blanchard, D.C., and A.H. Woodcock. (1957). Bubble formation and modification in the sea and its meteorological significance, Tellus, 9, 145-158. https://doi.org/10.3402/tellusa.v9i2.9094

Cole, I. S., Paterson, D. A., &Ganther, W. D. (2003). Holistic model for atmospheric corrosion Part 1 - theoretical framework for production, transportation and deposition of marine salts. *Corrosion Engineering, Science and Technology*, 38(2), 129–134. https://doi.org/10.1179/147842203767789203

Fang, G., Lin, S., Chang, S., Chou, C. (2009). Effect of typhoon on atmospheric particulates in autumn in central Taiwan. *Atmos. Environ*. 43, 6039e6048.https://doi.org/10.1016/j.atmosenv.2009.08.033

Feng, L., Shen, H., Zhu, Y., Gao, H., & Yao, X. (2017). Insight into Generation and Evolution of Sea-Salt Aerosols from Field Measurements in Diversified Marine and Coastal Atmospheres. *Scientific Reports, 7(1).* https://doi:10.1038/srep41260

Fu, H. Y., Zheng, M., Yan, C. Q., Li, X. Y., Gao, H. W., Yao, X. H., et al. (2015). Sources and characteristics of fine particles over the Yellow Sea and Bohai Sea using online single particle aerosol mass spectrometer. *Journal*

of Environmental Sciences, 29, 62–70. https://doi.org/10.1016/j.jes.2014.09.031

Goyal, R., Sen Gupta, A., Jucker, M., & England, M. H. (2021). Historical and projected changes in the Southern Hemisphere surface westerlies. *Geophysical Research Letters*, 48(4), e2020GL090849. https://doi.org/10.1029/2020GL090849

Gong, S. L., Barrie, L. A., & Lazare, M. (2002). Canadian Aerosol Module (CAM): A size-segregated simulation of atmospheric aerosol processes for climate and air quality models 2. Global sea-salt aerosol and its budgets. *Journal of Geophysical Research: Atmospheres*, 107(D24). https://doi.org/10.1029/2001jd002004

Gruber, N., Landschutzer, P., &Lovenduski, N. S. (2019). The variable Southern Ocean carbon sink. *Annual Review of Marine Science*, 11(1), 159. https://doi.org/10.1146/annurev-marine-121916-063407

Jiang, B., Xie, Z., Lam, P. K. S., He, P., Yue, F., Wang, L., et al. (2021). Spatial and temporal distribution of sea salt aerosol mass concentrations in the marine boundary layer from the Arctic to the Antarctic. J*ournal of Geophysical Research: Atmospheres*, 126(6), e2020JD033892. https://doi.org/10.1029/2020JD033892

Lewis, E. R., & Schwartz, S. E. (2004). Sea salt aerosol production: Mechanisms, methods, 648 measurements, and models. American Geophysical Union. https://doi.org/10.1029/GM152

Li, L., Huang, Z., Dong, J., Li, M., Gao, W., Nian, H., Fu, Z., Zhang, G., Bi, X., Cheng, P.,Zhou, Z., (2011). Real time bipolar time-of-flight mass spectrometer for analyzing single aerosol particles. Int. J. Mass Spectrom. 303(2-3), 118e124. https://doi.org/10.1016/j.ijms.2011.01.017

Li L, Li M, Huang ZX, Gao W, Nian HQ, Fu Z, Gao J, Chai FH, Zhou Z. (2014). Ambient particle characterization by single particle aerosolmass spectrometry in an urban area of Beijing. *Atmos Environ* 94,323–331.https://doi.org/10.1016/j.atmosenv.2014.03.048

Liu, N., Fu, G., &Kuo, Y.-H. (2012). Statistical characteristics of austral summer cyclones in Southern Ocean. *Journal of Ocean University of China, 11*(2), 118-128. https://doi:10.1007/s11802-012-1828-7

Liu, S., Liu, C. C., Froyd, K. D., Schill, G. P., Murphy, D. M., Bui, T. P., . . . Gao, R. S. (2021). Sea spray aerosol concentration modulated by sea surface temperature. *Proc Natl Acad Sci U S A*, 118(9). https://doi.org/10.1073/pnas.2020583118

Ma, L., Li, M., Zhang, H., Li, L., Huang, Z., Gao, W., … Zhou, Z. (2016). Comparative analysis of chemical composition and sources of aerosol particles in urban Beijing during clear, hazy, and dusty days using single particle aerosol mass spectrometry. *Journal of Cleaner Production, 112, 1319–1329.*

McDonald, R. L., Unni, C. K., & Duce, R. A. (1982). Estimation of atmospheric sea salt dry deposition: Wind speed and particle size dependence. *Journal of Geophysical Research*, 87(C2), 1246.

https://doi.org/10.1029/JC087iC02p01246

McInnes, L. M., Quinn, P. K., Covert, D. S. & Anderson, T. L. (1996). Gravimetric analysis, ionic composition, and associated water mass of the marine aerosol. *Atmos. Environ.* 30, 869–884https://doi.org/10.1016/1352-2310(95)00354-1

McCoy, I. L., McCoy, D. T., Wood, R., Regayre, L., Watson-Parris, D., Grosvenor, D. P., … Gordon, H. (2020). The hemispheric contrast in cloud microphysical properties constrains aerosol forcing. *Proceedings of the National Academy of Sciences, 201922502.*https:// doi.org /10.1073/pnas.1922502117

Monahan, E. C., &Muircheartaigh, I. O. (1980). Optimal power-law description of oceanic whitecap coverage dependence on wind-speed. *Journal of Physical Oceanography*, 10(12), 2094–2099. https://doi.org/10.1175/1520-0485(1980)010<2094:Opldoo>2.0.Co;2

Monahan, E. C., D. E. Spiel, and K. L. Davidson. (1986). A model of marineaerosol generation via whitecaps and wave disruption, in Oceanic Whitecaps.*Oceanic Whitecaps*. https://doi.org/10.1007/978-94-009-4668-2_16

O'Dowd, C. D., & de Leeuw, G. (2007). Marine aerosol production: A review of the current knowledge. Philosophical Transactions of the Royal Society A: Mathematical, *Physical and Engineering Sciences*, 365(1856), 1753–1774. https://doi.org/10.1098/rsta.2007.2043

Pierce, J. R., & Adams, P. J. (2006). Global evaluation of CCN formation by direct emission of sea salt and growth of ultrafine sea salt. *Journal of Geophysical Research*, 111(D6), D06203. https://doi.org/10.1029/2005jd006186

Quinn, P. K. & Coffman, D. J. (1999). Comment on "Contribution of different aerosolspecies to the global aerosol extinction optical thickness: estimates from model results" by Tegen et al. *J. Geophys. Res.* 104, 4241–4248.https://doi.org/10.1029/1998JD200066

Quinn, P. K., & Bates, T. S. (2011). The case against climate regulation via oceanic phytoplankton sulphur emissions. *Nature*, 480(7375), 51–56. https://doi.org/10.1038/nature10580

Quinn, P. K., Coffman, D. J., Johnson, J. E., Upchurch, L. M., & Bates, T. S. (2017). Small fraction of marine cloud condensation nuclei made up of sea spray aerosol. *Nature Geoscience,* 10(9), 674–679. https://doi.org/10.1038/ngeo3003

Shi, J., Yan, J., Wang, S., Zhao, S., Zhang, M., Xu, S., . . . Yang, H. (2022). Determinant of sea salt aerosol emission in the Southern Hemisphere in summer time. *Earth and Space Science, 9*(11). https://doi.org/10.1029/2022ea002529

Stokes, M. D., Deane, G. B., Prather, K., Bertram, T. H., Ruppel, M. J., Ryder, O. S., et al. (2013). A marine aerosol reference tank system as a breaking wave analogue for the production of foam and sea-spray aerosols. *Atmospheric Measurement Techniques*, 6(4), 1085–1094. https://doi.org/10.5194/amt-6-1085-2013

Takemura, T., Nakajima, T., Dubovik, O., Holben, B. N., &Kinne, S. (2002). single-scattering albedo and radiative forcing of various aerosol species with a global three-dimensional model. *Journal of Climate, 15(4), 333–352.* https://doi.org/10.1175/1520-0442(2002)015<0333:ssaarf>2.0.co;2

Teinila, K., Frey, A., Hillamo, R., Tulp, H. C., & Weller, R. (2014). A study of the sea-salt chemistry using size-segregated aerosol measurements at coastal Antarctic station Neumayer. Atmospheric Environment, 96, 11–19. https://doi.org/10.1016/j.atmosenv.2014.07.025

Twomey, S. (1977). *The Influence of Pollution on the Shortwave Albedo of Clouds. Journal of the Atmospheric Sciences, 34(7), 1149–1152.*https://doi.org/10.1175/1520-0469(1977)034<1149:tiopot>2.0.co;2

Thomas, M. A., Devasthale, A., &Kahnert, M. (2022). Marine aerosol properties over the Southern Ocean in relation to the wintertime meteor-ological conditions. *Atmospheric Chemistry and Physics*, 22(1), 119–137.https://doi.org/10.5194/acp-22-119-2022

Toffoli, A., Loffredo, L., Le Roy, P., Lefèvre, J.-M., &Babanin, A. V. (2012). *On the variability of sea drag in finite water depth. Journal of Geophysical Research: Oceans, 117(C11),*https://doi.org/10.1029/2011jc007857f, https://doi.org/10.1175/JAS3766.1.

Xu, G. J., Gao, Y., Lin, Q., Li, W., & Chen, L. Q. (2013). Characteristics of water-soluble inorganic and organic ions in aerosols over the Southern Ocean and coastal East Antarctica during austral summer. *Journal of Geophysical Research: Atmospheres*, 118(23), 13303–13318. https://doi.org/10.1002/2013jd019496

Yan, J., Chen, L., Lin, Q., Zhao, S., & Zhang, M. (2016). *Effect of typhoon on atmospheric aerosol particle pollutants accumulation over Xiamen, China. Chemosphere, 159, 244–255.* doi:10.1016/j.chemosphere.2016.06.00

Yan, J. P., Chen, L. Q., Lin, Q., Zhao, S. H., Li, L., & Zhu, D. Y. (2017). Marine aerosol using on‐board aerosol mass spectrometry.*Environmental Science*, 38(7), 2629–2636. https://doi.org/10.13227/j.hjkx.201612065

Yan, J., Jung, J., Lin, Q., Zhang, M., Xu, S., & Zhao, S. (2020). Effect of sea ice retreat on marine aerosol emissions in the Southern Ocean, Antarctica. *Science of the Total Environment*, 745, 140773. https://doi.org/10.1016/j.scitotenv.2020.140773

Yeatman, S. G., Spokes, L. J., &Jickells, T. D. (2001). Comparisons of coarse‐mode aerosol nitrate and ammonium at two polluted coastalsites. *Atmospheric Environment*, 35(7), 1321– 1335. https://doi.org/10.1016/S1352-2310(00)00452-0

Young, L. H., Li, C. H., Lin, M. Y., Hwang, B. F., Hsu, H. T., Chen, Y. C., et al. (2016). Field performance of a semi-continuous monitor for ambient PM2.5 water-soluble inorganic ions and gases at a suburban site.

Atmospheric Environment, 144, 376–388. https://doi.org/10.1016/j.atmosenv.2016.08.062

475

Figures/Tables

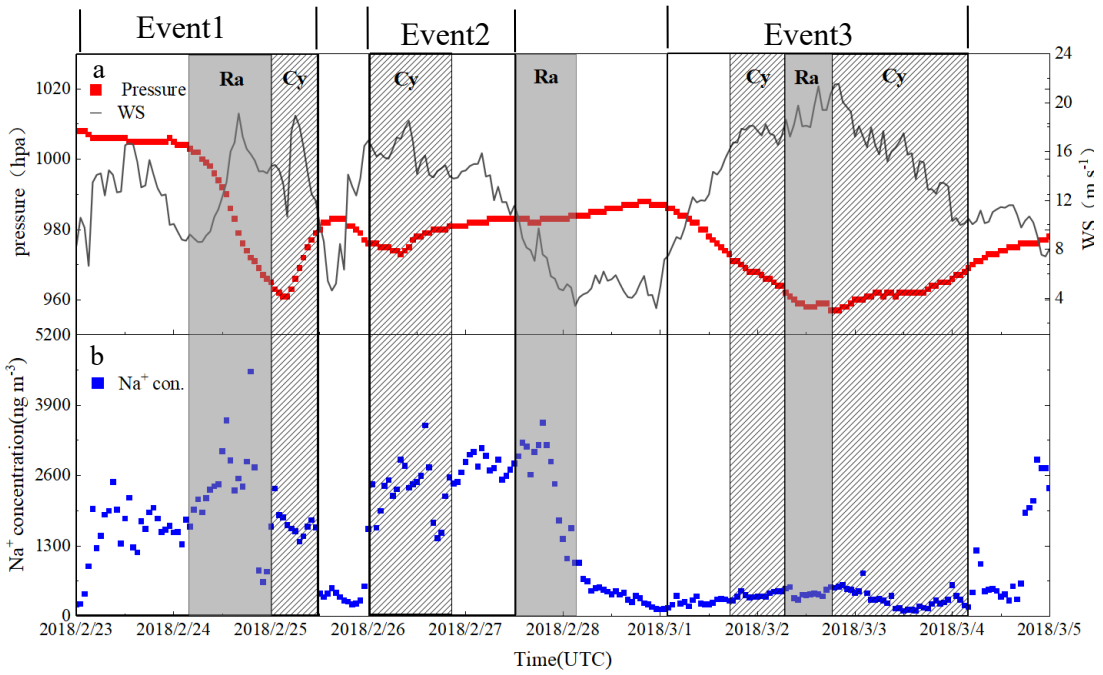

Figure 1. Temporal distributions of Na^+ and relevant meteorological parameters obtained during the period 23 February to 4 March 2018 in the cyclone area of the Southern Ocean. (a) Time series of atmospheric pressure (hpa) and wind speed (WS. m s^{-1}). (b) Time series of Na^+ concentrations (ng m^{-3}). Shading indicates: Ra - precipitation periods; Cy - cyclone periods. No shading corresponds to non-cyclone periods.

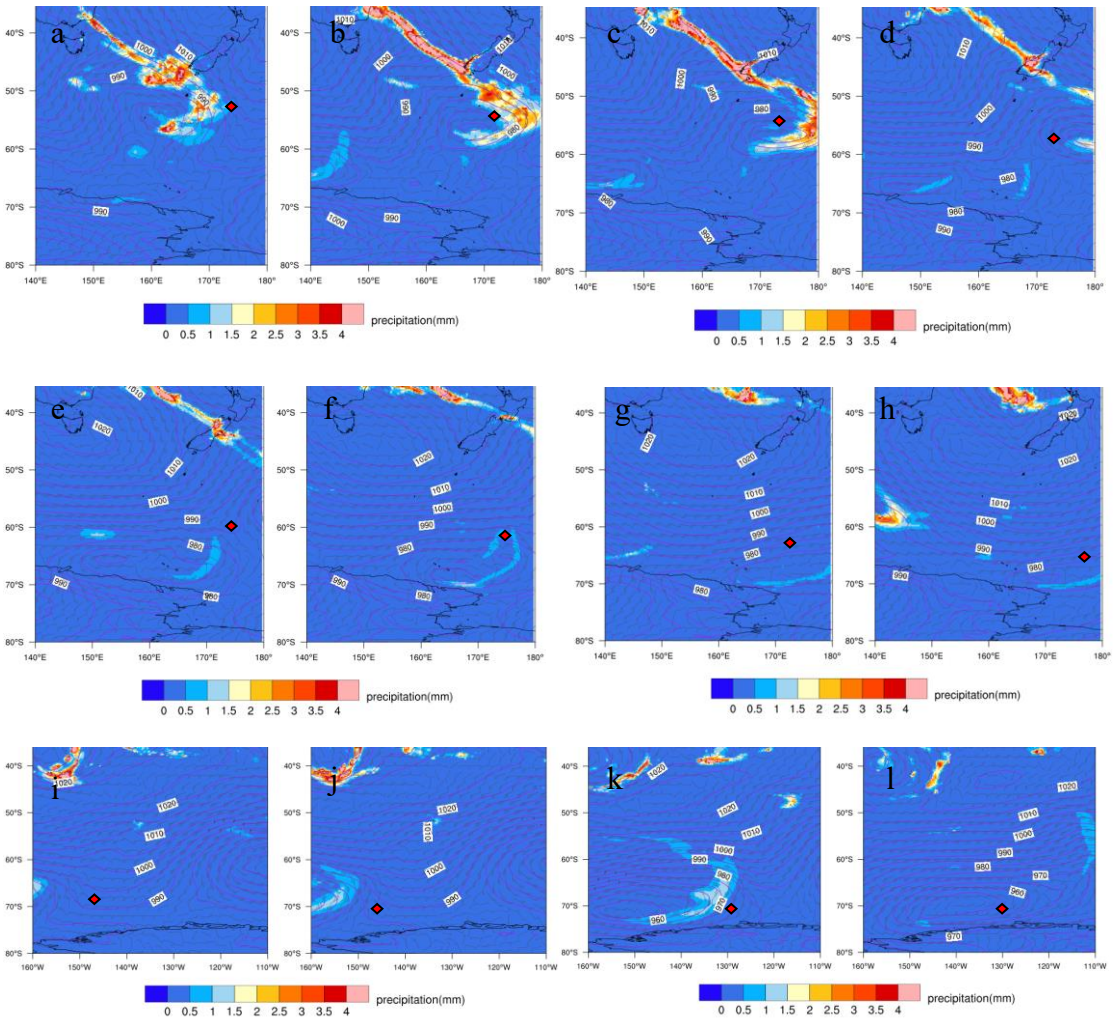

Figure 2. Sea surface pressure (hpa) and total precipitation (mm) maps for the three observed cyclone events. Event 1: (a) 14:00 24/2/18; (b) 20:00 24/2/18; (c) 01:00 25/2/18; (d) 08:00 25/2/18. Event 2: (e) 16:00 25/2/18; (f) 00:00 26/2/18; (g) 20:00 26/2/18; (h) 18:00 26/2/18. Event 3: (i) 01:00 1/3/18 (j) 18:00 1/3/18 (k) 13:00 2/3/18; (l) 22:00 2/3/18. The red diamond represents the position of the research ship. All times are UTC. The coastline of Antarctica is seen at the bottom of each figure.

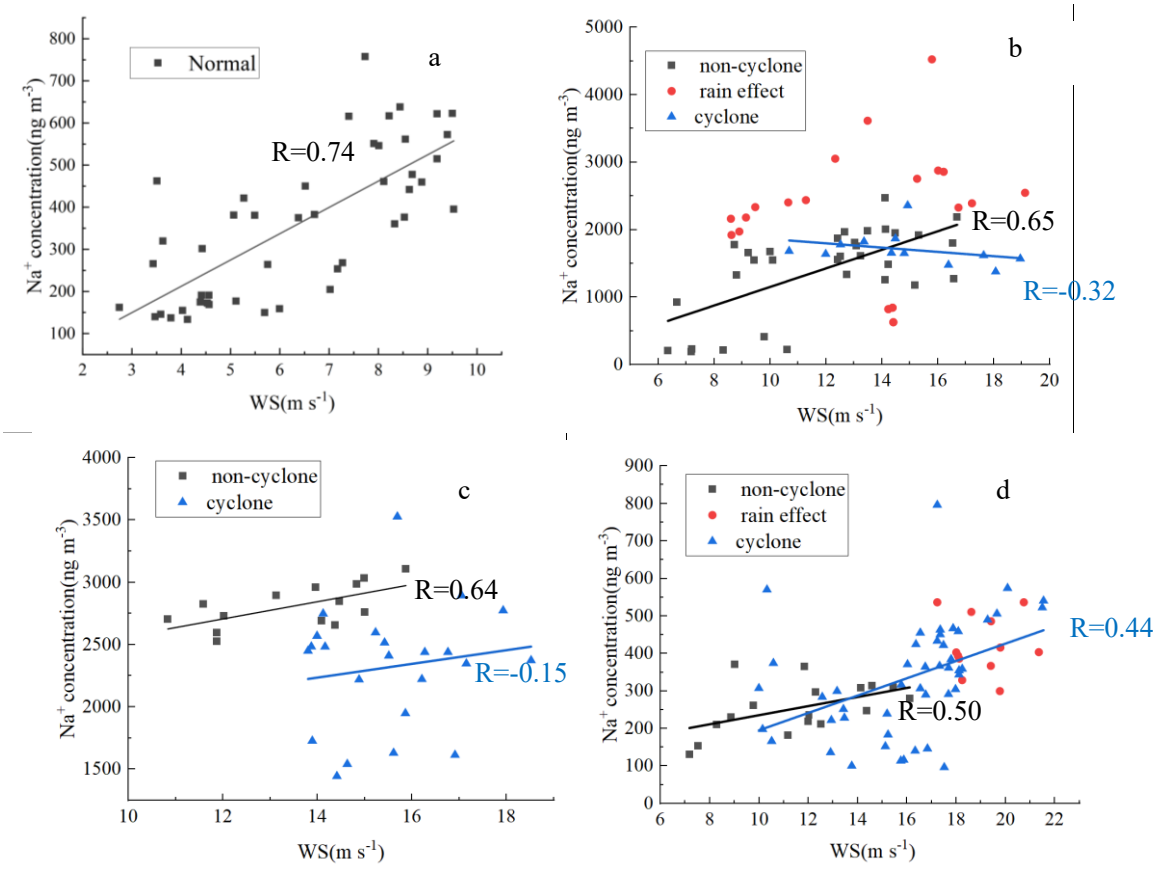

Figure 3. Correlation between Na^+ concentration and wind speed under different meteorological conditions. (a) A non-cyclone "normal" period (i.e., stable air pressure and relative humidity, constant air mass, no precipitation). (b) Event 1 (cyclone, non-cyclone and raining periods). (c) Event 2 (cyclone and non-cyclone periods). (d) Event 3 (cyclone, non-cyclone and raining periods).

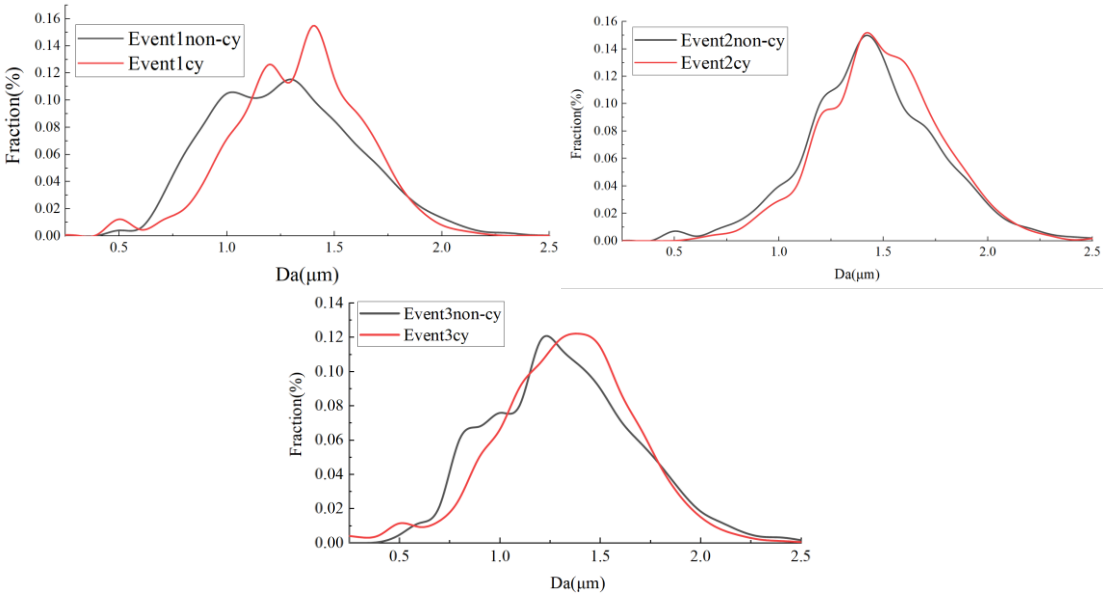

Figure 4. SSA size distributions (in terms of fractional percent) for cyclone and non-cyclone periods during the three observed Events.

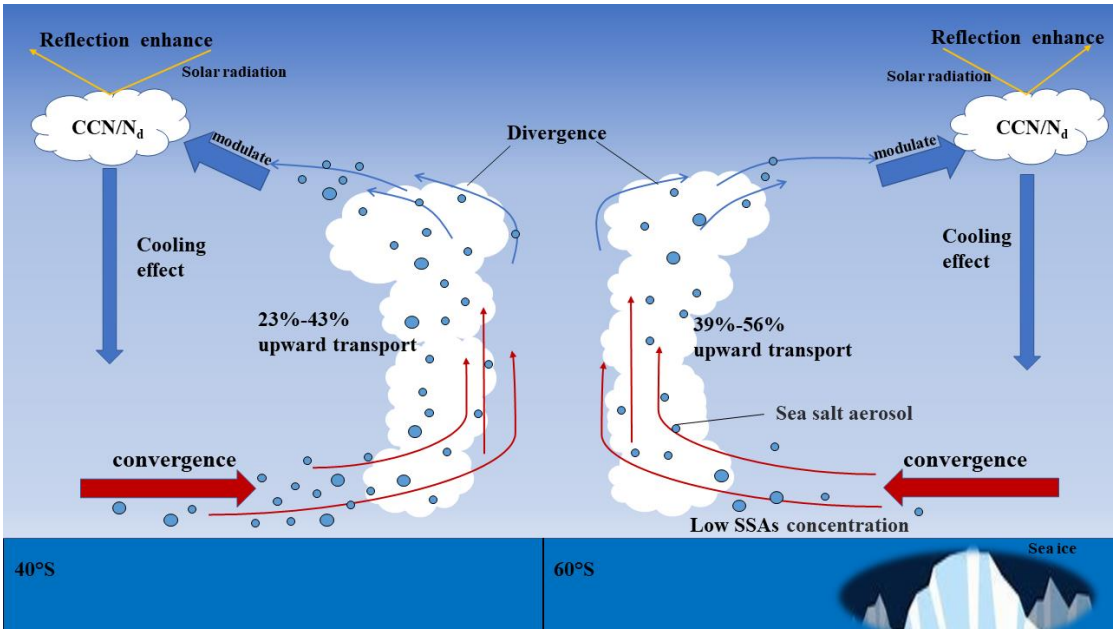

Figure 5. Schematic diagram illustrating the impact of cyclone on SSA generation and transport and the resulting climate effects.

515

Table 1. Estimation of SSAs vertical transport proportion by assessing the difference of wind stress and Sea-salt flux.

	Event 1	Event 2	Event 3
Quotient of wind stress	1.689	1.310	2.153
Quotient of sea-salt flux	2.156	1.463	3.031
Average Na^+ con. (non-cy) ng/m^3	1273.19	2816.90	254.76
Average Na^+ con. (cy) ng/m^3	1647.31	2353.74	334.94
Estimated U-$SSA_{(wind\ stress)}$ con. ng/m^3	2151.05	3689.30	548.52
Estimated U-$SSA_{(Sea\text{-}salt\ flux)}$ con. ng/m^3	2745.16	4113.74	772.14
Estimated upward transport $_{(wind\ stress)}$	23.4%	36.2%	38.9%
Estimated upward transport $_{(Sea\text{-}salt\ flux)}$	39.9%	42.8%	56.6%